Hyperosmolarity enhances the lung capillary barrier

Zeenat Safdar,[1,2] Ping Wang,[1] Hideo Ichimura,[1] Andrew C. Issekutz,[3] Sadiqa Quadri,[1] and Jahar Bhattacharya[1]

[1]Lung Biology Laboratory and
[2]Division of Pulmonary–Critical Care Medicine, St. Luke's–Roosevelt Hospital Center, College of Physicians and Surgeons, Columbia University, New York, New York, USA
[3]Department of Pediatrics, Dalhousie University, Halifax, Nova Scotia, Canada

Although capillary barrier deterioration underlies major inflammatory lung pathology, barrier-enhancing strategies are not available. To consider hyperosmolar therapy as a possible strategy, we gave 15-minute infusions of hyperosmolar sucrose in lung venular capillaries imaged in real time. Surprisingly, this treatment enhanced the capillary barrier, as indicated by quantification of the capillary hydraulic conductivity. The barrier enhancement was sufficient to block the injurious effects of thrombin, TNF-α, and H_2O_2 in single capillaries, and of intratracheal acid instillation in the whole lung. Capillary immunofluorescence indicated that the hyperosmolar infusion markedly augmented actin filament formation and E-cadherin expression at the endothelial cell periphery. The actin-depolymerizing agent latrunculin B abrogated the hyperosmolar barrier enhancement as well as the actin filament formation, suggesting a role for actin in the barrier response. Furthermore, hyperosmolar infusion blocked TNF-α–induced P-selectin expression in an actin-dependent manner. Our results provide the first evidence to our knowledge that in lung capillaries, hyperosmolarity remodels the endothelial barrier and the actin cytoskeleton to enhance barrier properties and block proinflammatory secretory processes. Hyperosmolar therapy may be beneficial in lung inflammatory disease.

J. Clin. Invest. **112**:1541–1549 (2003). doi:10.1172/JCI200318370.

Introduction

The lung capillary barrier critically regulates fluid flux into lung tissue. Failure of the barrier, as in lung inflammation, leads to pulmonary edema and other serious clinical consequences (1, 2). The endothelial cell is the major cell type constituting the barrier, and receptor- and stress-mediated endothelial signaling are the principal mechanisms underlying barrier failure (3). However, little is known regarding the mechanisms that strengthen the barrier or promote barrier recovery following injury. Although these mechanisms are likely to be important from a therapeutic standpoint, they remain entirely unaddressed in the pulmonary circulation.

Here, because of its possible anti-inflammatory effects, we consider the barrier-repair potential of blood hyperosmolarity. Hyperosmolar infusions, which are commonly applied in resuscitation therapy (4), suppress lung injury (5–8), inhibit expression of endothelial leukocyte adhesion molecules (8, 9), and block the proinflammatory effects of lipopolysaccharide (8). Furthermore, hyperosmolar infusions expand blood volume (10, 11) and cause hemodilution (10), suggesting that the capillary barrier remains intact despite the potential cell-shrinkage effect of hyperosmolarity (12). However, the endothelial mechanisms underlying these protective hyperosmolar effects remain unknown.

We recently reported that in cultured endothelial monolayers, hyperosmolar exposure increases membrane E-cadherin expression and augments formation of cortical actin filaments (13). As these findings suggest a barrier enhancing effect of hyperosmolarity, we tested the hypothesis by infusing hyperosmolar sucrose in lung venular capillaries. To assess barrier properties, we applied our split-drop technique, which provides sensitive barrier quantification in terms of the capillary hydraulic conductivity (Lp) (14–16). We also determined the increase in filtration rate at a fixed capillary pressure of 3 cmH_2O (ΔJv), as ΔJv denotes barrier deterioration (15). In addition, we determined expression of the leukocyte adhesion receptor P-selectin, which in lung venular capillaries marks an endothelial proinflammatory response (17). We report here our novel findings that hyperosmolar infusions enhanced capillary barrier properties and blocked P-selectin expression.

Methods

Solutions and reagents. Except where specified otherwise general reagents were purchased from Sigma Aldrich (St. Louis, Missouri, USA) and fluorescent reagents, from Molecular Probes Inc. (Eugene, Oregon, USA). Isosmolar Ringer's buffer contained: 144 mM Na^+; 1.5 mM Ca^{2+}; 123 mM Cl^-; 28 mM lactate, at pH 7.4 (pH Meter;

Received for publication March 17, 2003, and accepted in revised form September 22, 2003.

Address correspondence to: Jahar Bhattacharya, St. Luke's–Roosevelt Hospital Center, 1000 10th Avenue, New York, New York 10019, USA. Phone: (212) 523-7310; Fax: (212) 523-8005; E-mail: jb39@columbia.edu.

Conflict of interest: The authors have declared that no conflict of interest exists.

Nonstandard abbreviations used: hydraulic conductivity (Lp); increase in filtration rate at a fixed capillary pressure of 3 cm H_2O (ΔJv); milliosmole (mosm); split-drop volume (V); filtration rate (Jv); capillary pressure (Pc); interstitial pressure (Pinst).

Beckman Instruments, Irvine, California, USA). Hyperosmolar buffer (350 milliosmole [mosm]) was prepared by adding sucrose or urea to Ringer's buffer. All buffers contained 4% albumin (essentially fatty acid free). TNF-α (human recombinant; Calbiochem, La Jolla, California, USA) was prepared in PBS. Genistein (4′,5,7-trihydroxyisoflavone) latrunculin B, and jasplakinolide were prepared in isosmolar Ringer's buffer containing DMSO (0.01%). Saponin (0.1%) (ICN Biomedicals Inc., Aurora, Ohio, USA) was prepared in Ringer's buffer containing 1% FBS and 4% dextran (70 kDa). Formaldehyde (3.7%) was prepared in PBS. Antibodies used were anti-P-selectin mAb RP-2 (17), an anti-E-cadherin mAb (13) (Transduction Laboratories Inc., Lexington, Kentucky, USA), and Alexa-Fluor 488–conjugated goat anti-mouse secondary Ab.

Lung perfusion and microscopy. Our methods of preparing and imaging isolated blood-perfused rat lungs have been described (17–19). Briefly, lungs excised from adult male Sprague-Dawley rats were continuously pump-perfused (10–12 ml/min) with autologous rat blood warmed to 37°C. The pulmonary artery and left atrial pressures were maintained at 10 and 3 cmH_2O respectively. Airway pressure was held constant at 5 cmH_2O during micropuncture. Lungs were given cyclic inflations occasionally to prevent alveolar collapse. For real-time microscopy, the lungs were placed on a vibration-free table and viewed by stereo microscopy (SZH; Olympus America Inc., Melville, New York, USA), epifluorescence microscopy (AX-70; Olympus America Inc.), or confocal microscopy (Pascal LSM; Carl Zeiss, Thornwood, New York, USA). All data were obtained from venular capillaries (20–30 μm in diameter) that lie immediately downstream of the alveolar septum (14, 15). To avoid leukocyte effects, we maintained blood-free conditions in the experimental capillaries by infusing isosmolar Ringer's buffer containing 4% albumin through a wedged venous microcatheter (17). This catheter was also used for infusing reagents and dyes.

For epifluorescence microscopy, fluorophores were excited using mercury arc lamp illumination directed through appropriate interference filters (XB58/25R and XB62/25R; Omega Optical Inc., Brattleboro, Vermont, USA) and filter sets (71000, 41001, and 41004; Chroma Technology Corp., Brattleboro, Vermont, USA). Fluorescence emissions were collected through an objective lens (LUMPlanFL 40X/0.8W; Olympus Optical, Melville, New York, USA) and an image intensifier (Midnight Sun; Imaging Research Inc., St. Catharines, Ontario, Canada), and were captured with a charge-coupled device camera (CCD-72; Dage MTI, Michigan City, Indiana, USA). Both epifluorescence and confocal images were subjected to image analysis (MCID 5; Imaging Research Inc.).

Immunofluorescence. Infusions were given through a venous catheter to fix (3.7% formaldehyde in PBS, pH 7.4, 10 minutes, 37°C) and permeabilize (saponin 0.1%, 5 minutes) single capillaries. To determine the fluorescence of F-actin we infused rhodamine-phalloidin (5 units/ml; 10 minutes), and then rinsed the capillary with buffer infusions. To determine fluorescence of E-cadherin or P-selectin, we infused anti-E-cadherin mAb (10 minutes) or mAb RP-2 (4 minutes), respectively. For both, we followed with 2-minute infusions of the fluorescent secondary Ab's and, finally, with buffer to remove unbound fluorescence.

Split-drop technique. Transcapillary filtration rates were determined by our described split-drop technique (14–16). Briefly, an oil drop is microinjected into the capillary and then split with a test solution (vehicle: isosmolar Ringer's buffer containing 4% albumin). As the test solution filters across the capillary wall, the distance (split length) between the two segments of the split oil drop, hence the split-drop volume (V), progressively decreases. From measurements made from video recordings, split-drop volume is plotted against time and filtration rate (Jv) is calculated in terms of the surface area of filtration. The slope of the line relating Jv to capillary pressure (Pc) at two levels of Pc gives Lp. The stability of the preparation was established by ensuring that baseline Lp values obtained in the first 30–50 minutes of lung perfusion fell in the range of our previous baseline data (15). The split-drop procedure takes less than 2 minutes.

We have previously developed the theoretical principles underlying Jv determination by the split-drop technique (14). According to these principles, for constant Jv, loss of split-drop volume (V) across the walls of a cylindrical capillary is described by the first-order relation $-Jv\,(t) = -dV/dt = (\pi \times D^2) \times (dL/dt)/4$, where t is time, D is capillary diameter and L is split-drop length. It can be shown (14) that if Jv is constant, integration of the first equation gives $-Jv.t = (D/4) \times \ln(V/Vo)$, where V_0 is the initial split-drop volume. Defining the constant k as $(D/4) \times \ln(V/V_0)$, the second equation becomes the exponential $(V/V_0) = e^{-kt}$. Experimentally, the relationship in this third equation is confirmed by the exponential changes in the split-drop volume that we have reported several times (14, 20) and that we replicated here (Figure 1a). Jv is determined from the third equation by estimating k from exponential regression and then differentiating at $t = 0$. A potential error in this estimate of Jv may be attributable to changes in filtration forces during the volume transient.

Interstitial pressure determinations. We have extensively reported our methods for lung interstitial pressure (Pinst) determinations (21–23). Briefly, after a single venular capillary is viewed under bright-field microscopy the pericapillary interstitial space is micropunctured by means of glass micropipettes (tip diameter, 3 μm) connected to a servo-null pressure measurement system (Model 5A; Instrumentation for Medicine, San Diego, California, USA). Zero for the micropressure system is obtained by immersing the pipette tip in a saline pool lying immediately above the pleural surface. All determinations meet our acceptability criteria, namely that the Pinst reading must be stable for at least 1 minute, and that zero levels must match both before and after the determination. All pressure recordings are referred to the level of micropuncture.

Acid-instilled lung injury. We held anesthetized (pentobarbital, 30 mg/kg intraperitoneally) rats (Sprague-Dawley; body weight, 500–600 g) in a supine and inclined position on a thermal blanket (Harvard Apparatus Inc., Holliston, Massachusetts, USA) set at 37°C. Through a femoral vein catheter we infused either hyperosmolar sucrose or isosmolar Ringer's buffer at 4 ml/kg for 15 minutes. To determine plasma osmolarity (Model 210 osmometer; Advanced Instruments Inc., Norwood, Massachusetts, USA), we obtained blood samples from the femoral vein immediately prior to starting the infusion, and then at 15, 30, and 120 minutes after beginning the infusion. Within a minute of starting the femoral vein infusion, we instilled through a tracheotomy cannula either a bolus of 0.1 N HCl in saline or saline alone at 2 ml/kg. After obtaining the final femoral blood sample, we opened the chest and cross-clamped the lungs at the hilum. After excising the lungs, we determined the blood-free, extravascular lung water content by the wet-dry method, which is standard in our laboratory (24).

Statistics. All data are reported as mean ± SD; n = number of capillaries; and data are from at least three capillaries from two lungs. Paired observations were compared using a paired Student's t test, and grouped differences were compared with ANOVA (Newman-Keuls test). Significance was accepted at $P < 0.05$.

Results

Barrier responses. Although Lp was unaffected by a 15-minute infusion of isosmolar Ringer's buffer (300 mosm) (Figure 1b), a similar infusion of hyperosmolar sucrose (350 mosm) markedly decreased Lp (Figure 1c), thus indicating the barrier protective effect of sustained hyperosmolar infusion. However, 15-minute infusions of different osmolarities revealed a U-shaped Lp response in which Lp decreased progressively with an increase in osmolarity from 300 to 350 mosm, although it increased at higher osmolarities (Figure 1d). As the protective effect was optimal at 350 mosm, we used this concentration for further experiments. In a single experiment, we confirmed our previous finding that a 1-minute infusion of hyperosmolar sucrose increases Lp (Figure 1c, dashed line between stars) (15). Taking these 1- and 15-minute responses to 350 mosm together, our interpretation is that the barrier effect occurred in a time-dependent and biphasic matter, as indicated by the fact that in that early barrier deterioration was followed by barrier enhancement.

As the Lp determination required several micropuncture steps, for rapid barrier quantification we obtained single measurements of Jv at a fixed Pc of 3 cmH_2O. Although in the untreated capillary the liquid flux was absorptive (Figure 2a, left), a 1-minute hyperosmolar challenge increased Jv and converted the flux direction to filtration (Figure 2a, middle). This flux reversal at a constant Pc denotes barrier deterioration (15). Accordingly, barrier protection was evident in that the same challenge given at the end of a 15-minute hyperosmolar infusion re-established absorption (Figure 2a, right). Accordingly, increases in Jv (ΔJv) at baseline (Figure 2b, gray bars), or after a 15-minute isosmolar infusion (Figure 2b, white bars), denoted barrier deterioration due to a 1-minute infusion of hyperosmolar sucrose, thrombin, TNF-α, or H_2O_2. However, these barrier-deteriorating responses were each abrogated following a 15-minute hyperosmolar infusion (Figure 2b, black bars). In contrast, 15-minute hyperosmolar infusions of the membrane-permeable osmolyte urea failed to block the barrier-deteriorating effects of the 1-minute hyperosmolar challenge, and of TNF-α (Figure 2c), indicating that barrier protection was specific to hyperosmolar sucrose.

To assess intracellular mechanisms, we coinfused the F-actin depolymerizer latrunculin B, the F-actin stabilizer jasplakinolide, and the tyrosine kinase inhibitor genistein together with 15-minute isosmolar or hyperosmolar infusions (Figure 2d). Each agent increased ΔJv under isosmolar conditions, indicating that the agents may have induced nonspecific barrier effects. After 15-minute infusions of either DMSO in 4% albumin or 4% albumin alone, at Pc = 3 cmH_2O, Jv was identical (n = 3), which is consistent with reported findings that at the present concentration of 0.01% DMSO does not deteriorate the capillary barrier (25). However, the hyperosmolar barrier protection was blocked by latrunculin B and genistein, but not by jasplakinolide (Figure 2d). In capillaries given a 15-minute isosmolar infusion containing jasplakinolide, TNF-α failed to increase ΔJv

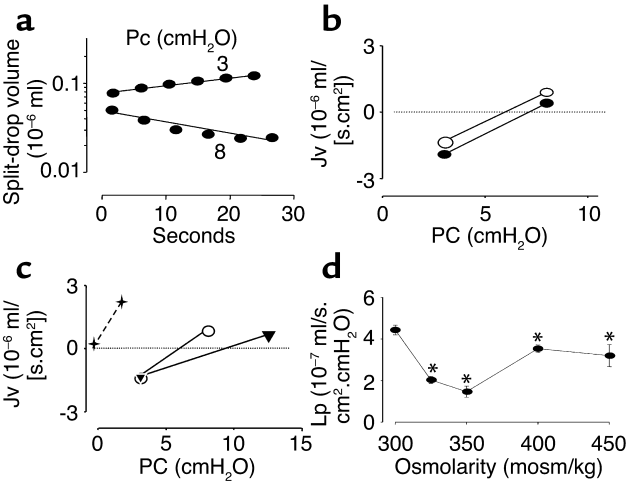

Figure 1
Barrier quantification in lung venular capillaries. (**a**) Semilogarithmic plots of split-drop volume versus time from single capillaries in which the oil drop was split with 4% albumin at the indicated Pc (numbers above and below lines). (**b** and **c**) Plots are data from single capillaries given no infusion (open circles), or a 15-minute infusion of isosmolar Ringer's buffer (300 mosm; filled circles), and a 1-minute (stars) or 15-minute (filled triangles) infusion of hyperosmolar sucrose (350 mosm). The corresponding Lp values (10^{-7} ml/s × cm^2 × cmH_2O) were 4.4, 5, 9, and 1.5. (**d**) Group data show Lp responses at baseline (300 mosm) and after 15-minute sucrose infusions of different osmolarites. Mean ± SD; n = 3, each point. *$P < 0.05$ compared with baseline.

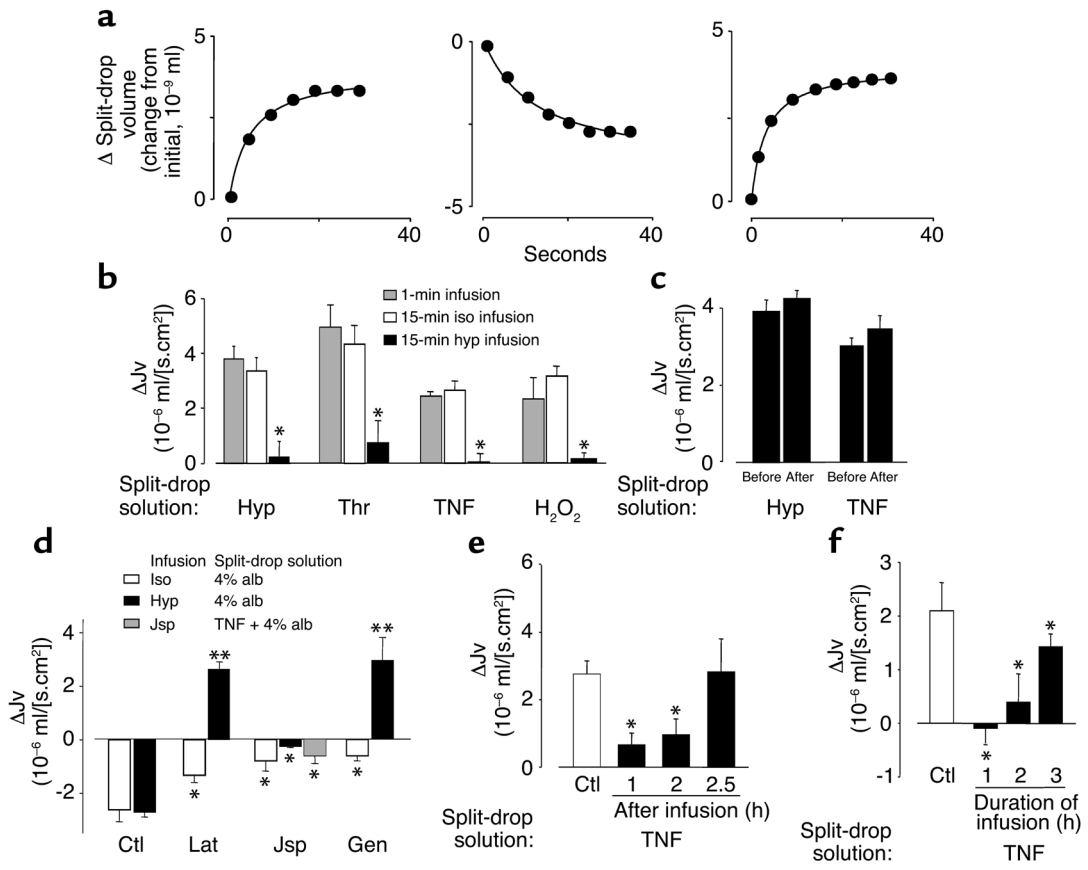

Figure 2
Split-drop filtration rates in lung capillaries. (**a**) Plots are data from single capillaries held at Pc = 3 cmH_2O. Infusion conditions are none (left), or hyperosmolar sucrose for 1 minute (middle) or 15 minutes (right). Δ split-drop volume, change from initial split-drop volume. (**b**) Data are responses to barrier-enhancing agonists in relation to the indicated infusion conditions. *$P < 0.05$ as compared with bar on immediate left. (**c**) Responses before and after hyperosmolar urea infusion (450 mosm). (**d**) Barrier responses in capillaries given 15-minute infusions with agents as indicated or with no agent (control [ctl]). Split-drop responses were obtained following infusion. *$P < 0.05$ compared with control; **$P < 0.05$ compared with isosmolar condition. (**e**) Responses to TNF-α before (control) and after 15-minute hyperosmolar infusion at indicated periods. *$P < 0.05$ compared with control. (**f**) Responses to TNF-α before (control) and after hyperosmolar infusions of different durations. *$P < 0.05$ compared with control. For determination of filtration rate, the oil drop was split by the indicated agents in 4% albumin (split-drop solution). Mean ± SD; $n = 3$, each bar. iso, isosmolar Ringer's buffer (300 mosm); hyp, hyperosmolar sucrose (350 mosm); thr, thrombin (7 units/ml); TNF, TNF-α (200 ng/ml); H_2O_2 (100 μM); jsp, jasplakinolide (100 nM) alb, albumin; lat, latrunculin B (100 nM); gen, genistein (50 μM).

above control (Figure 2d, gray bar), indicating that the barrier was protected by F-actin stabilization. We have discussed these results below.

To assess the duration of hyperosmolar barrier protection, we quantified ΔJv at different time points. After the 15-minute hyperosmolar infusion, the protective effect for TNF-α was sustained for up to 2 hours (Figure 2e). Hyperosmolar infusions given for 1–3 hours were also barrier protective, although the effect was weaker at 3 hours than at the earlier time points (Figure 2f).

To determine interstitial effects of capillary infusions, we determined Pinst by the micropuncture–servo-null technique using our reported protocol (22, 23). As this approach allows stable readings for 1- to 2-minute durations we repeated the determinations in the space immediately adjacent to the venular capillary several times during infusions. Pinst was slightly subatomospheric in the absence of infusion (not shown) and remained unchanged after a 15-minute isosmolar infusion (Figure 3a, left tracing). We have previously reported similar Pinst under baseline conditions (23). However, after the 15-minute hyperosmolar infusion, Pinst not only decreased (Figure 3a, right tracing) but also continued to decrease while we maintained the infusion (Figure 3, b and c). Furthermore, increasing Pc in the range for Lp determinations did not modify Pinst (Figure 3c). These findings rule out a role for Pinst increases in the barrier effect demonstrated here.

Endothelial morphology. To define the actin role further, we stained capillaries for F-actin using rhodamine-phalloidin. Under isosmolar conditions, actin fluorescence was weak even at high camera gain (Figure 4a). However, the 15-minute hyperosmolar challenge markedly increased the fluorescence (Figure 4b), and the response was inhibited by both

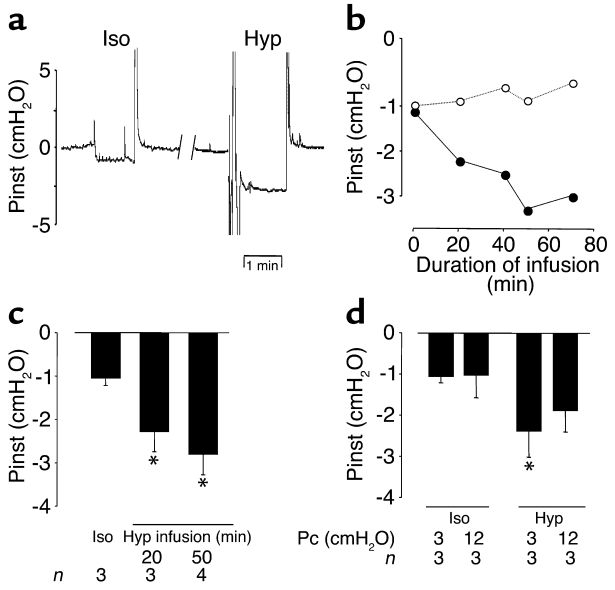

Figure 3
Interstitial pressure determinations by the micropuncture–servo-null method in rat lung. (**a**) Pressure tracings obtained after the indicated 15-minute infusions. Zero pressure was established by removal of the micropipette from the interstitium into a saline pool. (**b**) Single experiment data during isosmolar (open circles) and hyperosmolar (filled circles) infusion. (**c**) Group data show responses after isosmolar infusion and after the indicated periods of hyperosmolar infusion. (**d**) Effect of Pc on Pinst after indicated 15-minute infusions. Mean ± SD; $n = 3$, each bar; $^*P < 0.05$ as compared with isomolar function. iso, isosmolar Ringer's buffer (300 mosm); hyp, hyperosmolar sucrose (350 mosm).

latrunculin B and genistein (Figure 4c). When given alone, jasplakinolide, but not latrunculin B or genistein, augmented actin fluorescence (Figure 4c).

Confocal microscopy of hyperosmolarity-treated capillaries revealed consistently greater rhodamine fluorescence at branch-points especially around ostia of tributary vessels (Figure 5a, top, arrow). Optical sections taken along a vertical axis indicated that as tributaries progressively merged with the mainstream capillary, the intensity of actin fluorescence progressively decreased (Figure 5a, middle and bottom, arrows). In general, actin fluorescence was higher at tributary branch-points than at midsegmental locations lacking branch-points altogether (Figure 5b), indicating that the hyperosmolar actin response was spatially different within the same capillary.

To define the cell junction further, we loaded hyperosmolarity-treated capillaries with fluo 4, the Ca^{2+}-sensing cytosolic dye and viewed cells at high magnification. Fluo 4 fluorescence was bright in the nuclear region, but became attenuated toward the cell periphery (Figure 5c), thereby providing an approximate location of the cell junction. At these sites of attenuated fluo 4 fluorescence, we detected fluorescence of the adherens junction protein E-cadherin (Figure 5c), which thus marked the endothelial junction. The hyperosmolarity-induced actin response was now evident as spots of rhodamine fluorescence that colocalized with E-cadherin (Figure 5c), confirming the endothelial junction as the site of actin filament enhancement.

Not shown are data indicating weak capillary fluorescence for actin and E-cadherin under control conditions, and undetectable fluorescence for either the VE-cadherin mAb, or the secondary Ab given alone. Also not shown are data from single experiments in which we determined that the 15-minute hyperosmolar treatment caused no increases in fluo 4 fluorescence, although H_2O_2 increased the fluorescence as expected (18). Hence, hyperosmolar exposure did not increase endothelial Ca^{2+}.

P-selectin expression. As in our previous studies (17, 18), P-selectin expression was almost undetectable in these capillaries at baseline (Figure 6a, left), but was strongly induced by TNF-α (Figure 6a, middle). However, the 15-minute hyperosmolar infusion markedly inhibited

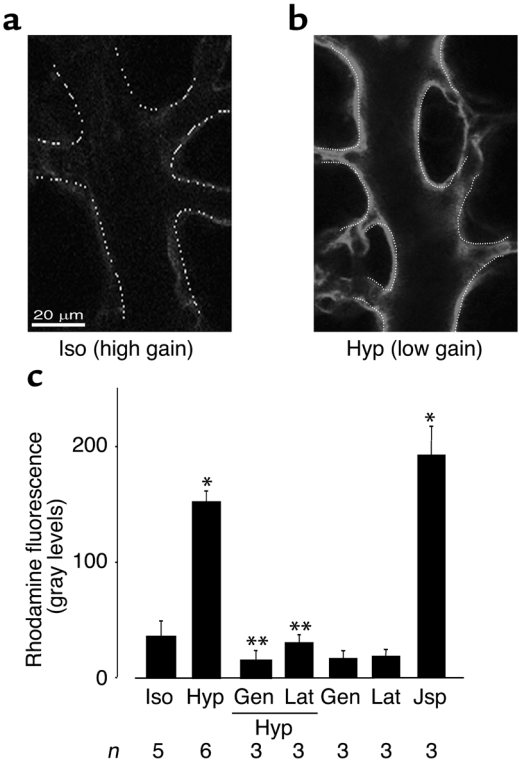

Figure 4
Confocal microscopy of actin fluorescence in lung capillaries. (**a** and **b**) Images show single capillaries that received 15-minute infusions as indicated. Camera gain was set as shown. Red pseudocolor reflects fluorescence of rhodamine-phalloidin. Replicated four times. (**c**) Bars represent responses to infusions of isosmolar buffer and hyperosmolar sucrose given alone, hyperosmolar sucrose given with genistein (gen; 50 μM) or latrunculin B (lat; 100 nM), and genistein, latrunculin B, or jasplakinolide (jsp; 100 nM) given alone. Mean ± SD; *n*, number of experiments. $^*P < 0.05$ compared with isosmolar infusion; $^{**}P < 0.05$ compared with hyperosmolar infusion. iso, isosmolar Ringer's buffer (300 mosm); hyp, hyperosmolar sucrose (350 mosm).

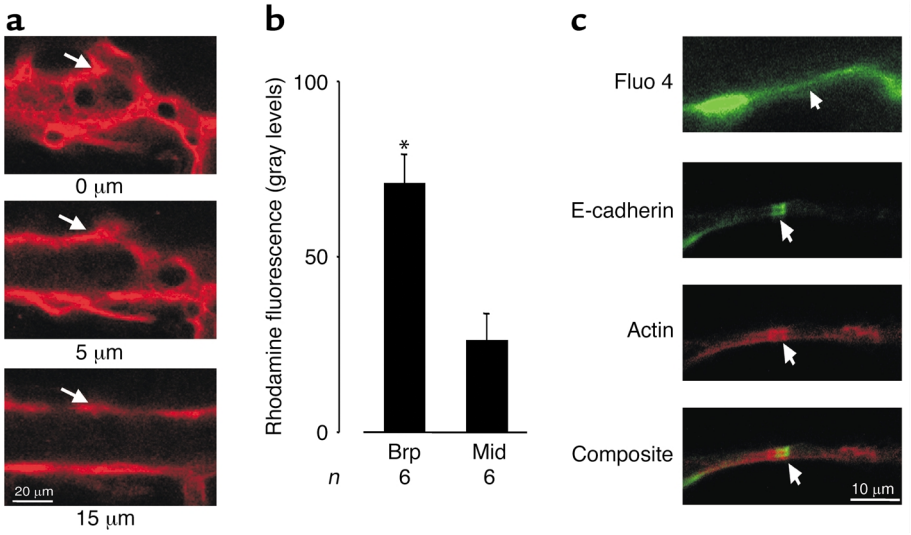

Figure 5
Spatial distribution of rhodamine-phalloidin fluorescence in lung capillaries. (**a**) Images are optical sections at indicated depths from top of a lung capillary given a 15-minute hyperosmolar infusion. Red pseudocolor shows actin fluorescence. A branch-point is indicated (arrows). Replicated four times. (**b**) Rhodamine fluorescence was quantified in a 4-μm^2 window placed over the capillary image at branch-point (brp) and midsegmental (mid) locations. Mean ± SD; *n*, number of experiments. *P < 0.05 compared with mid-segment. (**c**) Images show fluorescence of single endothelial cells in situ. The fluorophores are indicated. Arrows point to the cell periphery. The bottom image merges the E-cadherin and actin images. Replicated three times.

this TNF-α-induced effect (Figure 6, a and b). Latrunculin B given in the infusion reversed the hyperosmolar inhibition in a dose-dependent manner, whereas jasplakinolide replicated the hyperosmolar effect (Figure 6b). Infusion of latrunculin B or jasplakinolide alone did not augment P-selectin expression (Figure 6b). These findings indicated that actin stabilization blocked P-selectin exocytosis.

Anesthetized rat. In rats, we assessed acid-induced lung injury in terms of the extravascular lung water content. We instilled either acid or saline (2 ml/kg) in the trachea in the presence of 15-minute intravenous infusions of either hyperosmolar sucrose or isosmolar Ringer's solution. The hyperosmolar, but not the isosmolar, infusion transiently increased plasma osmolarity by 66 ± 12 mosm/kg (Figure 7a). In saline-instilled groups, lung water content was slightly higher than in noninstilled groups (Figure 7b, P < 0.05), indicating that the instilled liquid was not completely cleared in 2 hours (26, 27). However, lung water content was similar for groups treated with isosmolar and hyperosmolar infusions (Figure 7b, compare second and third bars), indicating that hyperosmolar infusion itself was not injurious. Acid instillation markedly increased lung water content above the saline-instilled control in animals given isosmolar infusion (Figure 7b, compare fourth bar with second bar), but not in animals given hyperosmolar infusion (Figure 7b, compare fifth bar with third bar). Taken together, these findings indicated that hyperosmolar infusion blocked acid-induced lung injury.

Discussion

Our major finding was that a 15-minute infusion of hyperosmolar sucrose markedly strengthened barrier properties in the lung capillary, as evident in the decrease in Lp and inhibition of the barrier-deteriorating effects of thrombin, TNF-α, and H_2O_2. The barrier protection was sustained for 2 hours and was optimally developed with hyperosmolarity of 350 mosm. Although Lp decreased progressively as we increased osmolarity in the 300- to 350-mosm range for reasons that are unclear, the effect weakened at higher osmolarities. Hyperosmolar infusions that were more prolonged were also barrier protective, although the protective effect tended to weaken as we increased the duration of infusion. As the capillaries were blood free (see Methods), we may discount leukocyte-induced effects as having a role in these responses. Taken together, these findings are the first evidence to our knowledge that a 15-minute hyperosmolar infusion in lung venular capillaries provides short-term barrier protection against permeability-enhancing agents.

Vascular infusions could increase tissue fluid accumulation, thereby increasing Pinst and reducing the ΔJv response. We ruled out this possibility through direct Pinst determinations; however, surprisingly, the 15-minute hyperosmolar infusion progressively decreased Pinst. Although mechanisms are not clear, it is possible that the enhanced absorptive flux induced by the hyperosmolar infusion (Figure 2c) reduced water content in the pericapillary space. This is consistent with our previous finding that reduction of interstitial water content decreases Pinst (23). Accordingly, in the absence of enhanced absorption, as during isosmolar infusion, Pinst was unaffected.

A striking set of capillary responses to hyperosmolarity were the fivefold increases in both actin polymerization and in the expression of the prototypic endothelial barrier protein E-cadherin that marks the adherens junction (28). We identified single endothelial cells by the cytosolic fluorescence of fluo 4, the Ca^{2+}-sensing dye. Fluo 4 fluorescence was nonresponsive to hyperosmolarity, thus ruling out a role for Ca^{2+} here. Attenuations of fluo 4 fluorescence marked the cell periphery. At this location, high-magnification images revealed actin and E-cadherin as colocalized

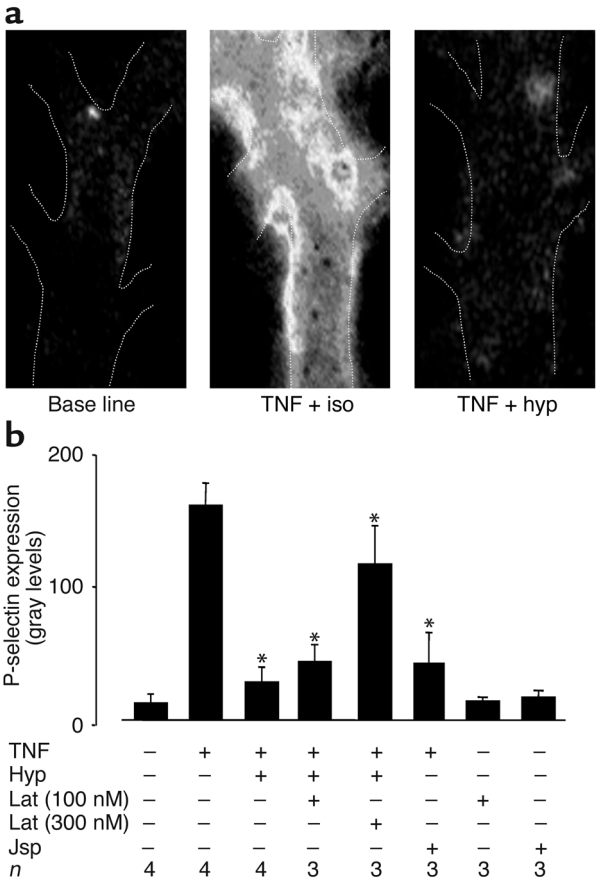

Figure 6
P-selectin expression in lung venular capillaries. (**a**) Images of single capillaries show P-selectin fluorescence at baseline, and that induced by TNF-α (200 ng/ml) after a 15-minute infusion of isosmolar Ringer's buffer (iso) or hyperosmolar (hyp) sucrose. Replicated four times. (**b**) Bars are group responses under the indicated conditions. TNF, TNF-α (200 ng/ml); hyp, 15-minute infusion hyperosmolar sucrose (350 mosm); lat, latrunculin B (100 or 300 nM); jsp, jasplakinolide (100 nM). Mean ± SD; *n*, number of experiments. **P* < 0.05 compared with second bar from left.

fluorescent spots. This colocalization is consistent with the known linkages of the cytoplasmic domains of cadherins through intermediate proteins, such as the catenins, to cortical actin (29, 30). VE-cadherin was undetectable in these capillaries, indicating that the dominant cadherin type in these capillaries was E-cadherin. These findings indicate that in these capillaries the major effects of hyperosmolarity were to remodel cortical actin and enhance E-cadherin in the endothelial barrier. As E-cadherin recycles in 1–2 hours (31), loss of excess cadherin from the junctional membrane may explain the time-dependent abrogation of the barrier enhancement following the 15-minute hyperosmolar infusion.

Cortical actin forms a barrier to exocytosis in many secretory cell types (32–34). Stabilization of cortical actin with phalloidin or jasplakinolide blocks secretion (33), whereas actin-depolymerizing agents enhance secretion (32). To test this hypothesis in the context of inflammation, we considered the secretion of the proinflammatory leukocyte adhesion receptor P-selectin. Previously, we reported that P-selectin secretion is a characteristic TNF-α-induced response (17). However, here the effect was completely blocked by hyperosmolar treatment, although it was rescued by inhibition of the associated actin polymerization with latrunculin B. The TNF-α-induced P-selectin expression was also inhibited by jasplakinolide treatment. Taken together, these P-selectin inhibitions are consistent with the notion that stabilization of cortical actin forms a significant secretion barrier. We conclude that cortical actin polymerization was the effective event underlying the anti-inflammatory effect of vascular hyperosmolarity, as reflected in P-selectin expression.

Genistein, which abrogated the enhancements of actin and E-cadherin, also blocked the barrier strengthening, pointing to tyrosine kinase activation as the relevant signaling mechanism. In our previously reported

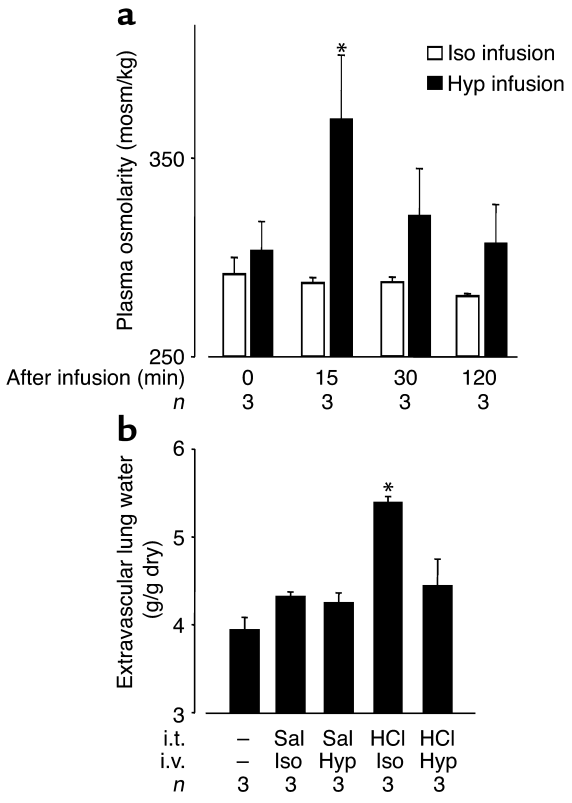

Figure 7
Effects of hyper- and isosmolar infusions in rats.(**a**) Data are for indicated time points after start of infusion. **P* < 0.05 compared with bar at 0 minutes. (**b**) Lung water content for groups given tracheal instillation and intravenous infusion as indicated. **P* < 0.05 compared with second bar. iso, isosmolar Ringer's buffer; hyp, hyperosmolar sucrose; i.v., intravenous infusion; i.t. intratracheal instillation; sal, saline; HCl, 0.1 N hydrochloric acid. Mean ± SD; *n*, number of experiments.

study a 1-minute hyperosmolar exposure both increased barrier permeability and induced tyrosine kinase activation (15). This early hyperpermeability response, which we replicated here, indicates that in the first minute of hyperosmolar exposure, the endothelial barrier weakens, possibly because endothelial cells shrink. In support of this hypothesis, hyperosmolar urea, which does not shrink endothelial cells, neither weakened the barrier in the first minute (15) nor, as we show here, established the subsequent barrier enhancement. Taking together our previous and present responses to 1- and 15-minute exposures to hyperosmolar sucrose we conclude that an initial, transient barrier-weakening preceded the barrier strengthening. It is possible that endothelial shrinkage early in the hyperosmolar response induces cell-matrix interactions that activate tyrosine kinases, which subsequently induce barrier strengthening. Thus, we reported previously that in cultured endothelial cells, hyperosmolar exposure causes tyrosine phosphorylation of the focal adhesion kinase, which leads to enhanced E-cadherin expression and barrier strengthening (13).

Actin has long been implicated in endothelial barrier regulation (3). Consistent with this understanding, latrunculin B alone caused a modest decrease in barrier properties. The combined presence of latrunculin B and hyperosmolarity caused marked barrier deterioration. Although this suggests a role for actin in hyperosmolar barrier enhancement, we cannot rule out the possibility that nonspecific effects were present. Such potential effects also complicate the interpretation of the jasplakinolide data. Thus, a comparison of the TNF data in Figure 2, b and c indicates that jasplakinolide was as effective as hyperosmolar infusion in protecting against TNF's barrier-deteriorating effect. However, given alone, jasplakinolide weakened the barrier, as indicated by the increase in ΔJv (Figure 2d). We suggest that the potential for nonspecific effects reduces the usefulness of these agents in interpreting the functional role of actin.

The association of endothelial barrier deterioration with actin depolymerization (35, 36) has established the view that cortical actin filaments stabilize endothelial barrier function. This view was challenged by recent studies involving the dominant negative and constitutively active forms of the small GTPase Rac1, which decrease and enhance cortical actin, respectively. Expression of either form of Rac1 fails to modify endothelial barrier responses to hyperosmolarity and thrombin (13, 37), indicating that barrier regulation under these conditions occurs independently of cortical actin. Although our findings are consistent with reports that hyperosmolarity induces actin polymerization in cultured endothelial cells (13), Chinese hamster ovary cells (38), and neutrophils (39), further studies are required to clarify actin's barrier-regulatory role.

To test the effectiveness of hyperosmolar barrier protection in an integrative setting, we exposed anesthetized rats to acid-instilled lung injury. In this widely reported model, the development of lung injury is indicated by an increase in the extravascular lung water content within 2–4 hours of intratracheal acid instillation (40, 41). Our findings are consistent with those reports in that in the control group, lung water content increased markedly 2 hours after acid instillation. However, in the presence of a 15-minute hyperosmolar infusion, the acid-induced lung injury was completely abolished. Although our findings suggest that hyperosmolar infusion is beneficial when given early in the onset of lung injury, further studies are required to evaluate the protective efficacy of hyperosmolar infusions given at different times after injury, for different durations, and at different osmolyte concentrations.

In conclusion, our studies bring into focus the role of endothelial cells in hyperosmolar barrier protection in lung capillaries. Our findings are consistent with several previous studies in which intravenous hyperosmolar infusions were reported to prevent lung injury (5–8). However, for the consideration of hyperosmolar infusion in clinical therapy, the role of the endothelium must be further clarified especially with regard to the manner in which barrier protection is initiated and is maintained in intact models of lung injury.

Acknowledgments

This work was supported by NIH grants HL-36024, HL-57556, HL-69514, and HL-64896 to J. Bhattacharya, and by a fellowship award to Z. Safdar from the Stony Wold-Herbert Fund Inc.

1. Luhr, O.R., et al. 1999. Incidence and mortality after acute respiratory failure and acute respiratory distress syndrome in Sweden, Denmark, and Iceland. The ARF Study Group. *Am. J. Respir. Crit. Care Med.* **159**:1849–1861.
2. Herridge, M.S., et al. 2003. One-year outcomes in survivors of the acute respiratory distress syndrome. *N. Engl. J. Med.* **348**:683–693.
3. Dudek, S.M., and Garcia, J.G. 2001. Cytoskeletal regulation of pulmonary vascular permeability. *J. Appl. Physiol.* **91**:1487–1500.
4. Tollofsrud, S., Mathru, M., and Kramer, G.C. 1998. Hypertonic-hyperoncotic solutions in open-heart surgery. *Perfusion.* **13**:289–296.
5. Coimbra, R., et al. 1997. Hypertonic saline resuscitation decreases susceptibility to sepsis after hemorrhagic shock. *J. Trauma.* **42**:602–606; discussion 606–607.
6. Rabinovici, R., Vernick, J., Hillegas, L., and Neville, L.F. 1996. Hypertonic saline treatment of acid aspiration-induced lung injury. *J. Surg. Res.* **60**:176–180.
7. Pascual, J.L., et al. 2003. Hypertonic saline resuscitation attenuates neutrophil lung sequestration and transmigration by diminishing leukocyte-endothelial interactions in a two-hit model of hemorrhagic shock and infection. *J. Trauma.* **54**:121–130; discussion 130–122.
8. Rizoli, S.B., et al. 1998. Immunomodulatory effects of hypertonic resuscitation on the development of lung inflammation following hemorrhagic shock. *J. Immunol.* **161**:6288–6296.
9. Ochi, H., Masuda, J., and Gimbrone, M.A. 2002. Hyperosmotic stimuli inhibit VCAM-1 expression in cultured endothelial cells via effects on interferon regulatory factor-1 expression and activity. *Eur. J. Immunol.* **32**:1821–1831.
10. Mazzoni, M.C., Borgstrom, P., Arfors, K.E., and Intaglietta, M. 1990. The efficacy of iso- and hyperosmotic fluids as volume expanders in fixed-volume and uncontrolled hemorrhage. *Ann. Emerg. Med.* **19**:350–358.
11. Tollofsrud, S., et al. 2001. The dynamics of vascular volume and fluid shifts of lactated Ringer's solution and hypertonic-saline-dextran solutions infused in normovolemic sheep. *Anesth. Analg.* **93**:823–831.
12. O'Donnell, M.E. 1993. Role of Na-K-Cl cotransport in vascular endothelial cell volume regulation. *Am. J. Physiol.* **264**:C1316–C1326.
13. Quadri, S.K., Bhattacharjee, M., Parthasarathi, K., Tanita, T., and Bhattacharya, J. 2003. Endothelial barrier strengthening by activation of focal adhesion kinase. *J. Biol. Chem.* **278**:13342–13349.

14. Bhattacharya, J. 1988. Hydraulic conductivity of lung venules determined by split-drop technique. *J. Appl. Physiol.* **64**:2562–2567.
15. Ragette, R., Fu, C., and Bhattacharya, J. 1997. Barrier effects of hyperosmolar signaling in microvascular endothelium of rat lung. *J. Clin. Invest.* **100**:685–692.
16. Qiao, R.L., and Bhattacharya, J. 1991. Segmental barrier properties of the pulmonary microvascular bed. *J. Appl. Physiol.* **71**:2152–2159.
17. Parthasarathi, K., Ichimura, H., Quadri, S., Issekutz, A., and Bhattacharya, J. 2002. Mitochondrial reactive oxygen species regulate spatial profile of proinflammatory responses in lung venular capillaries. *J. Immunol.* **169**:7078–7086.
18. Ichimura, H., Parthasarathi, K., Quadri, S., Issekutz, A.C., and Bhattacharya, J. 2003. Mechano-oxidative coupling by mitochondria induces proinflammatory responses in lung venular capillaries. *J. Clin. Invest.* **111**:691–699. doi:10.1172/JCI200317271.
19. Kuebler, W.M., Ying, X., Singh, B., Issekutz, A.C., and Bhattacharya, J. 1999. Pressure is proinflammatory in lung venular capillaries. *J. Clin. Invest.* **104**:495–502.
20. Qiao, R.L., Sadurski, R., and Bhattacharya, J. 1993. Hydraulic conductivity of ischemic pulmonary venules. *Am. J. Physiol.* **264**:L382–L386.
21. Glucksberg, M.R., and Bhattacharya, J. 1991. Effect of alveolar and pleural pressures on interstitial pressures in isolated dog lungs. *J. Appl. Physiol.* **70**:914–918.
22. Bhattacharya, J., Gropper, M.A., and Staub, N.C. 1984. Interstitial fluid pressure gradient measured by micropuncture in excised dog lung. *J. Appl. Physiol.* **56**:271–277.
23. Glucksberg, M.R., and Bhattacharya, J. 1989. Effect of dehydration on interstitial pressures in the isolated dog lung. *J. Appl. Physiol.* **67**:839–845.
24. Bhattacharya, J., Cruz, T., Bhattacharya, S., and Bray, B.A. 1989. Hyaluronan affects extravascular water in lungs of unanesthetized rabbits. *J. Appl. Physiol.* **66**:2595–2599.
25. Glass, C.A., and Bates, D.O. 2003. Role of endothelial Ca^{2+} stores in the regulation of hydraulic conductivity of Rana microvessels in vivo. *Am. J. Physiol. Heart Circ. Physiol.* **284**:H1468–H1478.
26. Sakuma, T., et al. 1997. Beta-adrenergic agonist stimulated alveolar fluid clearance in ex vivo human and rat lungs. *Am. J. Respir. Crit. Care Med.* **155**:506–512.
27. Fukuda, N., et al. 2001. Mechanisms of TNF-α stimulation of amiloride-sensitive sodium transport across alveolar epithelium. *Am. J. Physiol. Lung Cell. Mol. Physiol.* **280**:L1258–L1265.
28. Moy, A.B., et al. 2000. Histamine alters endothelial barrier function at cell-cell and cell-matrix sites. *Am. J. Physiol. Lung Cell. Mol. Physiol.* **278**:L888–L898.
29. Lampugnani, M.G., and Dejana, E. 1997. Interendothelial junctions: structure, signalling and functional roles. *Curr. Opin. Cell Biol.* **9**:674–682.
30. Conacci-Sorrell, M., Zhurinsky, J., and Ben-Ze'ev, A. 2002. The cadherin-catenin adhesion system in signaling and cancer. *J. Clin. Invest.* **109**:987–991. doi:10.1172/JCI200215429.
31. Le, T.L., Yap, A.S., and Stow, J.L. 1999. Recycling of E-cadherin: a potential mechanism for regulating cadherin dynamics. *J. Cell Biol.* **146**:219–232.
32. Rizoli, S.B., Rotstein, O.D., Parodo, J., Phillips, M.J., and Kapus, A. 2000. Hypertonic inhibition of exocytosis in neutrophils: central role for osmotic actin skeleton remodeling. *Am. J. Physiol. Cell Physiol.* **279**:C619–C633.
33. Klarenbach, S.W., Chipiuk, A., Nelson, R.C., Hollenberg, M.D., and Murray, A.G. 2003. Differential actions of PAR2 and PAR1 in stimulating human endothelial cell exocytosis and permeability: the role of Rho-GTPases. *Circ. Res.* **92**:272–278.
34. Chowdhury, H.H., Kreft, M., and Zorec, R. 2002. Distinct effect of actin cytoskeleton disassembly on exo- and endocytic events in a membrane patch of rat melanotrophs. *J. Physiol.* **545**:879–886.
35. Shasby, D.M., Shasby, S.S., Sullivan, J.M., and Peach, M.J. 1982. Role of endothelial cell cytoskeleton in control of endothelial permeability. *Circ. Res.* **51**:657–661.
36. Poli, A., Coleman, P.J., Mason, R.M., and Levick, J.R. 2002. Contribution of F-actin to barrier properties of the blood-joint pathway. *Microcirculation.* **9**:419–430.
37. Wojciak-Stothard, B., Potempa, S., Eichholtz, T., and Ridley, A.J. 2001. Rho and Rac but not Cdc42 regulate endothelial cell permeability. *J. Cell Sci.* **114**:1343–1355.
38. Di Ciano, C., et al. 2002. Osmotic stress-induced remodeling of the cortical cytoskeleton. *Am. J. Physiol. Cell Physiol.* **283**:C850–C865.
39. Lewis, A., Di Ciano, C., Rotstein, O.D., and Kapus, A. 2002. Osmotic stress activates Rac and Cdc42 in neutrophils: role in hypertonicity-induced actin polymerization. *Am. J. Physiol. Cell Physiol.* **282**:C271–C279.
40. Song, Y., et al. 2000. Role of aquaporins in alveolar fluid clearance in neonatal and adult lung, and in oedema formation following acute lung injury: studies in transgenic aquaporin null mice. *J. Physiol.* **525**:771–779.
41. Frank, J.A., et al. 2002. Low tidal volume reduces epithelial and endothelial injury in acid-injured rat lungs. *Am. J. Respir. Crit. Care Med.* **165**:242–249.